

Dynamic Analysis of Brushless DC Motor using Fuzzy Logic Controller

Jyotsna Niranjana¹, Varsha Mehar²,
^{1,2}Department of Electrical Engineering,
 RKDF University, Bhopal, India

Abstract—The advancement in the field of science, engineering and technology over last decades successfully designed brushless DC motor application possible in the automotive industry. This paper deals with one such technological advancements. In this dissertation, the brushless DC motors find huge applications in industries due to their high power density and ease of control. Usually, a three phase power semiconductor bridge is applied to control these motors. This dissertation report presents a fuzzy logic controller for speed control of a brushless DC motor by using. The fuzzy logic approach applied to speed control leads to an improved dynamic behavior of the motor drive system and an immune to load perturbations and parameter variations. The fuzzy logic controller is designed using based on a simple analogy between the control surfaces of the fuzzy logic controller and a given Proportional-Integral controller for the same application. Fuzzy logic control offers an improvement in the quality of the speed response, compared to PI control. This work focuses on investigation and evaluation of the performance of a brushless DC motor drive, controlled by PI, and fuzzy logic speed controllers. The Controllers are for the brushless DC motor drive simulated using MATLAB software package.

Keywords— Brushless DC Motor, Fuzzy Logic, PI Controller.

I. INTRODUCTION

Brushless DC (BLDC) motors are preferred as small horse-power control motors due to their high efficiency, silent operation, compact form, reliability, and low maintenance. However, the problems are encountered in these motor for variable speed operation over last decades continuing technology development in power semiconductors, microprocessors, adjustable speed drivers control schemes and permanent-magnet brushless electric motor production have been combined to enable reliable, cost-effective solution for a broad range of adjustable speed applications [1, 2].

Household appliances are expected to be one of fastest-growing end-product market for electronic motor drivers over the next few years. The major appliances include clothes washer's room air conditioners, refrigerators, vacuum cleaners, freezers, etc. Household appliance have traditionally relied on historical classic electric motor technologies such as single phase AC induction, including split phase, capacitor-start, capacitor-run types, and universal motor. These classic motors typically are operated at constant-speed directly from main AC power without regarding the efficiency. Consumers now demand for lower energy costs, better performance, reduced acoustic noise, and more convenience features. Those traditional technologies cannot provide the solutions [3, 4].

A. DC Motor Drives

DC motors used in rotor dynamics applications require precise and stable operation which is achieved by either speed or torque control. DC motors are usually free from harmonics, reactive power consumption and offer many more advantages [5]. Therefore, DC motors are widely used in fine speed controlled applications such as in rolling and paper mills. Due its high starting torque, series DC motor is best suited for traction applications like electric trains and cranes. Shunt DC motors are generally used for constant torque applications [6]. Figure 1 represents a basic structure of brushless DC motor drive with controller.

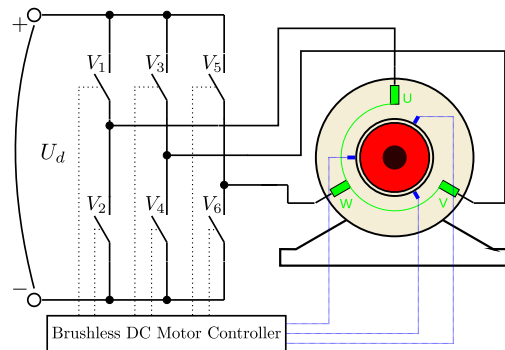


Fig. 1. Blushless DC Motor with Controller

One of the attractive features of the DC motor is that it offers a wide range of speed control both above and below the rated speeds [7, 8]. This can be achieved in shunt DC motors by methods such as armature control and field control. The series DC motor speed can be controlled by changing the terminal voltage. In spite of all these advantages, the DC motors also have some shortcomings: high initial cost, and operation and maintenance cost due to presence of commutator and brush gears [9].

Brushed DC motor should not be used in explosive and hazardous conditions because of sparks at the brush. In many applications permanent magnet, shunt wound and series wound are prominent components of DC motors. The Sommerfeld effect [10] characterization is done for all these motors and different speed control methods are described for passage of spin speed through the resonance frequency of the driven structure.

II. MATHEMATICAL MODELING OF BLDC MOTOR

The brushless DC motor is very similar to the standard wound rotor synchronous machine except that it has no damper windings and excitation is provided by a permanent magnet instead of a field winding. Since the rotor is made up of permanent magnet, saturation of magnetic flux linkage is same as that of synchronous machines [11]. The stator is having three phases winding and fed with the three phase source [12, 13]. Therefore the stator can be modeled by using the following equations. The voltage equation of BLDC motor can be represented as

$$\begin{bmatrix} V_a \\ V_b \\ V_c \end{bmatrix} = \begin{bmatrix} R & 0 & 0 \\ 0 & R & 0 \\ 0 & 0 & R \end{bmatrix} \begin{bmatrix} i_a \\ i_b \\ i_c \end{bmatrix} + \begin{bmatrix} L & 0 & 0 \\ 0 & L & 0 \\ 0 & 0 & L \end{bmatrix} \frac{d}{dt} \begin{bmatrix} i_a \\ i_b \\ i_c \end{bmatrix} + \begin{bmatrix} e_a \\ e_b \\ e_c \end{bmatrix} \quad (1)$$

where,

R = Phase Resistance,

L = Phase Inductance

V_a, V_b, V_c = Phase Voltages

i_a, i_b, i_c = Phase Currents

e_a, e_b, e_c = Back EMFs

The torque equation of the BLDC motor is as represented as in Equation 2

$$T = \frac{e_a i_a + e_b i_b + e_c i_c}{\omega} \quad (2)$$

where, ω is motor angular velocity.

The equation of the mechanical system is given by

$$T_e - T_l = J \frac{d\omega_m}{dt} + B\omega \quad (3)$$

where,

T_l = Load Torque [N-m]

J = Inertia of Rotor [kg-m²]

B = Damping Constant [N-ms-rad⁻¹]

III. RELATED WORK

A. Energy Cycle of Brushless DC Motor Chaotic System

Qi [14] transformed the original brushless DC motor (BLDCM) into the Kolmogorov type of system. Four types of torque have been revealed for vector field of the brushless DC motor (BLDCM) chaotic system. Accordingly, four forms of energy are identified for the system—kinetic, potential, dissipative, and supplied. The transforming relationship between kinetic energy and potential energy has been clarified for the system. Through an analogue of electrical and mechanical system, the electromechanical brushless DC motor (BLDCM) was regarded as a pure mechanical system. The rate of change of the Casimir function is the exchange power between dissipative energy and the supplied energy of the motor, which determines the behavior of orbit of the brushless DC motor (BLDCM).

1) *Mechanics of BLDCM Chaotic System:* The equations describing the non-salient-pole (or called round pole or smooth air gap) BLDCM can be written via a Park transformation [15, 16] as

$$Li_q = -Ri_q - nL\omega i_d - nk_t\omega + u_q \quad (4)$$

$$Li_d = -ri_d + nL\omega i_q + u_d \quad (5)$$

$$J\omega = nk_t i_q - b\omega - T_L \quad (6)$$

i_q is the quadrature-axis current, i_d the direct-axis current, and ω is the rotor velocity; R is the winding resistance, L_a is self-inductance of the winding with $L = \frac{3}{2}L_a$, n is the number of permanent-magnet pole pairs, k_e is the coefficient of the motor torque with $k_t = \sqrt{3/2}k_e$, J is the inertia of moment, b is the damping coefficient of bearing; u_q and u_d are the voltage across quadrature-axis and direct-axis, and T_L the external torque due to load.

The optimal, simple and analytical supremum bound of the brushless DC motor (BLDCM) chaotic attractor was identified through the Casimir function as well. Four cases analysis of the brushless DC motor (BLDCM) chaotic system in terms of combinations of four forms of energy further have been performed uncovering the insight and contributing factors of dynamics of periodic orbit, sink, and the chaotic attractors [17].

B. Adaptive Control Study for DC Motor using Meta-Heuristic Algorithms

Rodríguez-Molina *et al.* [18] implemented different optimization meta-heuristic techniques in the adaptive control that shows the qualities of each technique in solving the problem of online parameter estimation of a DC motor subject to parametric uncertainties. Among the analyzed qualities are the accuracy in speed regulation, the energy consumption, the invariability with respect to error and the computational time required for each technique. The simulation results show that AC-PSO (Ant Colony-Particle Swarm Optimization) and AC-DE (Ant Colony-Differential Evolution) are the most promising adaptive strategies [19].

The future velocity is estimated through a binomial crossover process where exchanges some components of the velocity equation ωx_i . This process is expressed in Equation 7, where CR is the probability of changing the current velocity and ω is a factor which reduce the velocity of all particles obtained within the range $[V_{min}, V_{max}]$.

$$x_{i,j}^{\text{next}} = \begin{cases} \omega v_{i,j} & \text{if } \text{rnd}(0,1) \leq CR \\ \omega x_{i,j} & \text{otherwise} \end{cases} \quad (7)$$

The future position is estimated as

$$x_i^{\text{next}} = x_i + x_{i-1}^{\text{next}} \quad (8)$$

Based on the obtained statistical results, a hybridization of the most promising meta-heuristic techniques is proposed and used in the adaptive control strategy. This alternative named as AC-PSO/DE (Ant Colony-Particle Swarm Optimization/Differential Evolution) has a significant performance

improvement with respect to the most promising adaptive strategies (AC-PSO and AC-DE) in the speed regulation of the DC motor.

C. Analysis of Dynamic Behavior of Direct Current Motor with Electrical Braking Techniques

Serteller *et al.* [20] compared three identical types of motor with their current, power and speed versus time characteristics including braking and decelerating. All of the results taken under certain loads indicates that shunt motor reverse current braking has an advantage among them because it has the quickest braking time. However, its power consumption does not have the lowest.

1) *Dynamic Equations of DC Motor:* The dynamic response of field winding excited and permanent magnet DC (PMDC) motor is governed by the following equations orderly:

$$\frac{d\omega_m}{dt} = \frac{1}{J}(T - T_L) \quad (9)$$

$$T = (k_e \phi) I_a \quad (10)$$

$$T_L = T + B\omega_m + T_c + c(\omega_m)^2 + T_S \quad (11)$$

$$E_a = (k_e \phi) \omega_m \quad (12)$$

$$\frac{dI_a}{dt} = \frac{1}{L_a}(V_a - I_a R_a - E_a) \quad (13)$$

$$\phi = \frac{N_f I_f}{\mathfrak{R}} = k_f I_f \quad (14)$$

$$\frac{dI_a}{dt} = \frac{1}{L_a}(V_a - I_a R_a - k_p \omega_m) \quad (15)$$

$$T = k_p I_a \quad (16)$$

Here ω_m is the angular speed (rad/s) of the motor (armature), T_L is the load torque, J is the moment of inertia. T is a magnitude of the motor electromagnetic torque. T defines the magnitude of the motor torque as a function of the resultant flux $\phi(Wb)$ within the machine taking into account field and armature flux (armature reaction). I_a is an armature current; k_e and k_p are constants for winding excited and PM, respectively. T_L defines the load torque components, in which B is a viscous damping coefficient, T_c is the coulomb frictional torque and c is a constant but ignored because of being small. T_S denoted as the standstill torque is taken of 0 Nm. V_a represents the terminal voltage. An Electro-motor force (emf) E_a is induced voltage within the armature winding. N_f is the number of field winding and \mathfrak{R} is the reluctance of the system [21–23].

D. Development of Wireless In-Wheel Motor Using Magnetic Resonance Coupling

Sato *et al.* [24] discussed the design, implementation and bench test results of a wireless-in wheel motor (W-IWM). An analysis of the stability of the wireless-in wheel motor (W-IWM) as a constant power load demonstrated the need

for control of the secondary-side voltage. To achieve this, a novel hysteresis control method was proposed.

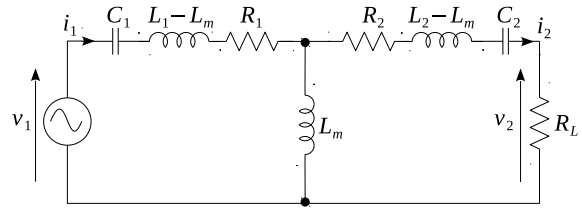


Fig. 2. Simplified Circuit for Wireless Power Transfer (WPT)

1) *Transmitter and Receiver Coil Design:* Figure 2 presents the simplified equivalent circuit of wireless power transfer (WPT). If it assumed to be fundamental power factor of secondary is unity, from the secondary rectifier to motor can be assumed genuine resistance [25]. Where, voltage amplifier ratio A_v and transmitting efficiency A_p can be assessed as follows:

$$A_v = \frac{V_2}{V_1} = j \frac{\omega_0 L_m R_{ac}}{R_1 R_{ac} + R_1 R_2 + (\omega_0 L_m)^2} \quad (17)$$

$$\eta = \frac{V_2 \bar{I}_2}{V_1 \bar{I}_1} = \frac{(\omega_0 L_m)^2 R_{ac}}{(R_L + R_2) \{R_1 R_{ac} + R_1 R_2 + (\omega L_m)^2\}} \quad (18)$$

The coil parameters R_1 , R_2 , and L_m , in Equation 18, are coil parameters that vary based on the coil size, number of turns, and coil misalignment. Where R_1 is primary coil resistance, R_2 is secondary coil resistance, and L_m is mutual inductance. According to the aforementioned conditions, equivalent resistance R_{ac} is calculated as follows:

$$R_{ac} = \frac{V_{21}^2}{P_2} \quad (19)$$

The relationships between V_{21} and V_{dc} is as follows:

$$V_{21} = \frac{2\sqrt{2}}{\pi} V_{dc} \quad (20)$$

When motor power outputs rated power, $R_{ac} = 30\Omega$. According to Equation 18, when $R_{ac} = 30\Omega$, the η is almost over 90%. As a result, the coils for the wireless-in wheel motor (W-IWM) can achieve high efficiency at rated power.

2) *Electric Power Conversion of Transmitter and Receiver:* The wireless-in wheel motor (W-IWM) is a permanent magnetic synchronous motor (PMSM) driven by a voltage type inverter and is assumed to have constant dc power. In order to analyze the stability of the secondary dc-link voltage, a simplified circuit model is introduced as shown in Figure 3. In this model, the primary circuit and the secondary converter are assumed to have an equivalent variable current source i_0 , which is the average output current of the secondary converter. The circuit equation of the simplified model is expressed as follows:

$$i_2 = i_0 - C_S \frac{dv_2}{dt} \quad (21)$$

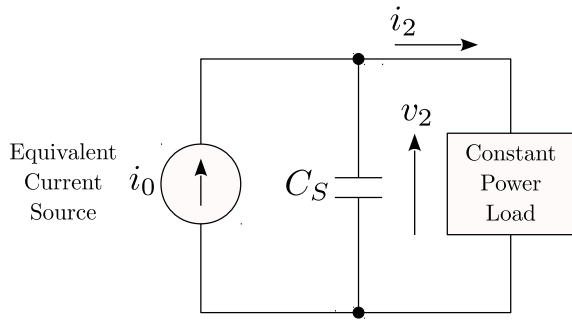


Fig. 3. Simplified Circuit Model

The load current i_2 is expressed as

$$i_2 = \frac{P_2}{v_2} \quad (22)$$

where P_2 is the load power. Substituting Equation 22 into 21

$$\frac{dv_2}{dt} = -\frac{p_2}{C_S v_2} + \frac{i_0}{C_S} \quad (23)$$

Linearizing Equation 23 around the equilibrium point

$$\frac{d\Delta v_2}{dt} = \frac{P_2 \Delta v_2}{C_S V_2^2} + \frac{\Delta i_0}{C_S} \quad (24)$$

$$v_2 = V_2 + \Delta v_2 \quad (25)$$

$$i_0 = I_0 + \Delta i_0 \quad (26)$$

Transfer function $P\Delta(s)$, which is from Δi_0 to Δv_2 , is derived by taking the Laplace transform of Equation 26 as follows:

$$P\Delta(s) = \frac{\Delta v_2(s)}{\Delta i_0(s)} = \frac{1}{C_S \left(s - \frac{P_2}{C_S V_2^2} \right)} \quad (27)$$

Then, the pole of $P\Delta(s)$, p is expressed as

$$p = \frac{P_2}{C_S V_2^2} \quad (28)$$

Therefore, $P\Delta(s)$ is unstable regardless of to the load power P_2 and the equilibrium point because $p_2 > 0$ and $V_2 > 0$. From the results of the aforementioned analysis, in the case of a constant power load, the load voltage is unstable, and stabilization control of the load voltage is necessary.

3) *Secondary DC-Link Voltage Control*: Figure 4 represents the block diagram of the W-IWM. In Figure 4, V_{batt} is the voltage of the battery of the EV. V_{batt} is inputted into the buck-boost converter, which converts V_{batt} to E , the DC voltage for the primary inverter. The reference for the primary inverter voltage, E^* , is calculated as

$$E^* = \frac{\pi}{4} \sqrt{2} V_1 \quad (29)$$

where,

$$V_1 = \frac{4}{\sqrt{2}\pi} E \sin\left(\frac{\pi}{2}\right) \quad (30)$$

From Equation 29, which is derived from V_{dc}^* and τ^* , which are, respectively, DC-link torque reference for the secondary

inverter and motor speed. Where the motor speed is provided to the primary side via Bluetooth communication. Wireless power transfer (WPT) coils means the control plant for the WPT. The secondary converter makes V_{dc} stable by using the hysteresis comparator. The motor is vector controlled by the secondary inverter.

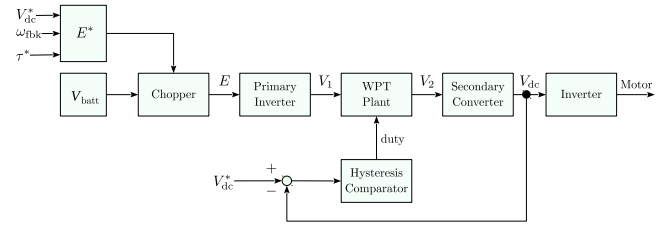


Fig. 4. Control Block Diagram of The Wireless-In Wheel Motor (W-IWM)

In addition, a feedforward control method [26] for the primary-side voltage, based on the output of the secondary-side converter estimated from motor speed and reference torque, was also proposed. The results of the bench tests conducted on the trial unit validated the effectiveness of the proposed control methods, showing high efficiency both when powering the motor and regenerating energy.

E. Dynamic Analysis and Chaos Suppression in a Fractional Order Brushless DC Motor

Rajagopal *et al.* [27] derived new results for the fractional order brushless DC (BLDC) motor. First, the dynamic properties of the fractional order brushless DC motor were discussed such as bifurcation with parameters, bifurcation with fractional orders, Lyapunov exponents [28, 29], and bi-coherence. Next, chaos control and stabilization of the fractional order brushless DC motor were achieved with three control schemes (sliding mode control, robust control and extended back-stepping control). The fractional order controller stability is established using Lyapunov stability theorem through a modified fractional order Lyapunov first derivative [30, 31]. Numerical simulations are established to illustrate the main results for the fractional order brushless DC motor.

The fractional order model of BLDC motor system is derived with the Caputo fractional order definition [32, 33], which is defined as

$$D_t^\alpha f(t) = \frac{1}{\Gamma(1-\alpha)} \int_{t_0}^t \frac{f(\tau)}{(t-\tau)^\alpha} d\tau \quad (31)$$

where α is the order of the system, t_0 and t are limits of the fractional order equation, and $f(t)$ is integer order calculus of the function.

For numerical calculations, Caputo-Riemann-Liouville fractional derivative [34, 35]. Thus, the equation (2) is modified as

$${}_{(t-L)}D_t^\alpha f(t) = \lim_{h \rightarrow 0} \left\{ h^{-\alpha} \sum_{j=0}^{N(t)} b_j (f(t-jh)) \right\} \quad (32)$$

Theoretically fractional order differential equations use infinite memory. Hence when we want to numerically calculate or

simulate the fractional order equations, finite memory principal will have to be used, where L is the memory length and h is the time sampling as

$$N(t) = \min \left\{ \left\lceil \frac{t}{h} \right\rceil, \left\lceil \frac{L}{h} \right\rceil \right\} \quad (33)$$

$$b_j = \left(1 - \frac{a + \alpha}{j} \right) b_{j-1} \quad (34)$$

Applying these fractional order approximations in to the integer order BLDC motor system, it yields the fractional order BLDC motor model described by Equation 35,

$$D^{\alpha_x} x = v_\alpha - x - yz + \rho z \quad (35)$$

$$D^{\alpha_y} y = v_d - \delta y + xz \quad (36)$$

$$D^{\alpha_z} z = \sigma(x - z) + \eta xy - T_L \quad (37)$$

where $\alpha_x, \alpha_y, \alpha_z$ are the fractional orders of the BLDC motor system.

F. Control Strategies for DC Motors Driving Rotor Dynamic Systems Through Resonance

Bisoi *et al.* [36] primarily focused on coasting up a rotor dynamic system mounted on flexible foundation to an operating speed above the structural resonance frequency. The rotor is assumed to be driven by a DC motor. It is found that the motor sizing needs to consider an estimate of the minimum power requirement to escape through the structural resonance, failing which the rotor speed may get captured at the resonance.

During passage through resonance, the consequential high amplitude vibrations can be reduced through different existing approaches that try to modify the mechanical structure such as using switched foundation stiffness, variable gear ratio in the motor, stick-slip and liquid dampers. However, structural modification is expensive and often infeasible. Another approach is to use heavy foundation damping. However, heavy foundation damping reduces the shock isolation capability of the flexible foundation. Therefore, the methods to promote passage through resonance by modifying the electrical parts of the DC motor were considered here. It was found that the best possible solution should deliver the peak motor power at the structural resonance frequency [37, 38]. The schematic circuit representation of field weakening control for series DC motor speed regulation above the rated operating speed is shown in Figure 5.

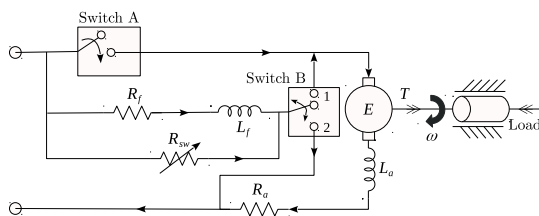


Fig. 5. Schematic Circuit of Field Weakening Resistor for Series DC Motor

In this regard, shunt motor configuration was found to be more appropriate. A switched control formalism combining the best properties from the shunt and series motor configurations was then proposed and validated through simulations.

IV. PROPOSED APPROACH

Fuzzy logic has rapidly become one of the most successful of today's technology for developing sophisticated control system. With it aid complex requirement so may be implemented in amazingly simple, easily minted and inexpensive controllers. The past few years have witnessed a rapid growth in number and variety of application of fuzzy logic. The application range from consumer products such as cameras, camcorder, washing machines and microwave ovens to industrial process control ,medical instrumentation, and decision-support system.

A. Proposed Fuzzy Logic Controller Model for Torque Ripple Minimization

Torque control of brushless DC motor drives has gained popularity in advanced motor drives applications since it offers fast instantaneous torque and flux control with simple implementation. This scheme is well known for its robustness in control as it is less dependency on machine parameters, does not need the complex field orientation block, speed encoder and the inner current regulation loop. Figure 6 represents a proposed fuzzy logic controller model for torque ripple minimization based on induction motor drive with a duty ratio fuzzy logic controller.

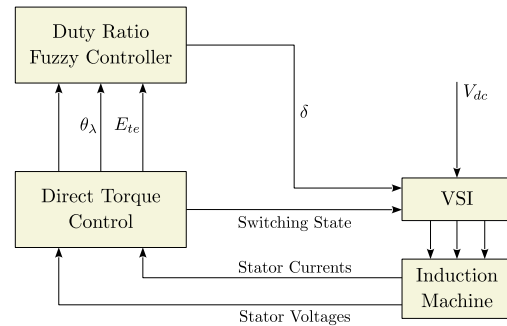


Fig. 6. Block Diagram for Proposed Fuzzy Logic Controller Model

V. RESULT ANALYSIS

The experimental setup of speed control of brushless dc motor shown in Figure V.

The experimental and simulation results with a speed reference input of 700rpm with a load torque of 0.6 N-m. In experimental are shown in Figure V and Figure V. The rotor is standstill at time zero with onset of the speed reference, the speed error, torque reference, and attains maximum value. The current is made to follow the reference by the current controller.

The speed response of the BLDC drive system using and PI controller and fuzzy logic controller. With the motor at rest, the reference speed is set at 75rad/s (700rpm) with

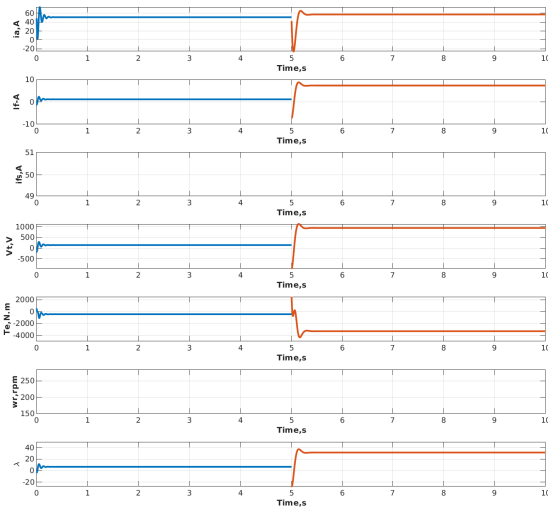


Fig. 7. Torque Analysis Case-1 (Armature Current, Shunt Field Current, Series Field Current, Output voltage, Electromechanical Torque, Speed, Flux Linkage vs Time)

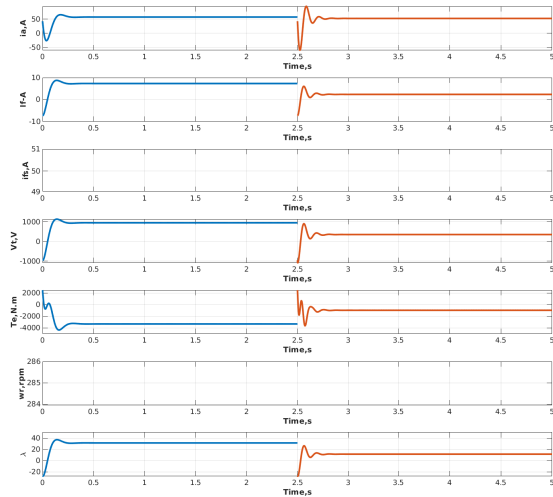


Fig. 9. Torque Analysis Case-3 (Armature Current, Shunt Field Current, Series Field Current, Output voltage, Electromechanical Torque, Speed, Flux Linkage vs Time)

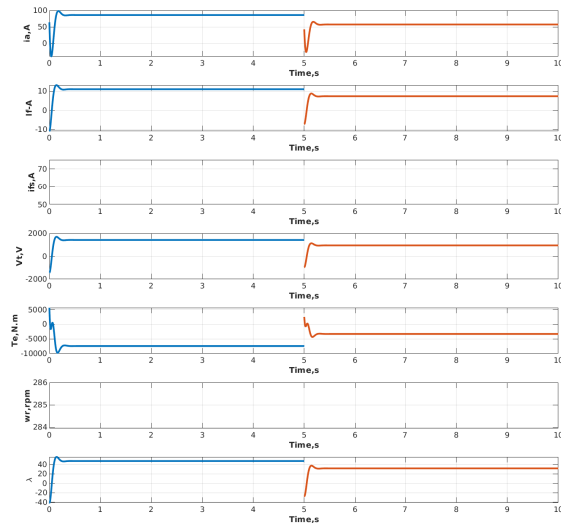


Fig. 8. Torque Analysis Case-2 (Armature Current, Shunt Field Current, Series Field Current, Output voltage, Electromechanical Torque, Speed, Flux Linkage vs Time)

a settling time 0.05 seconds the motor speed reaches the reference speed with a percentage overshoot of 6.667 with PI speed controller. The phase currents at the time starting getting transient due to initial phase back emfs machine are zero. After the speed reaching reference speed, phase currents are reaches the reference current. Phase currents are conduction with 120 angle duration shown in Figure V.

For FLC the motor speed reaches reference speed with

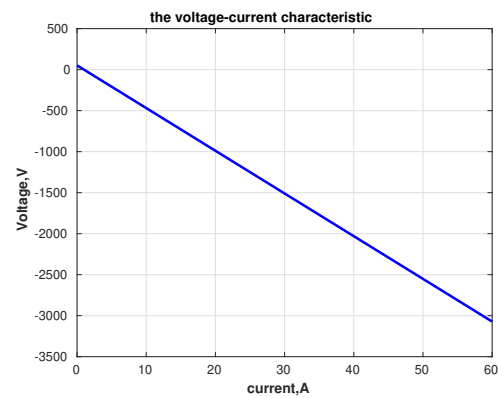


Fig. 10. V-I Characteristics

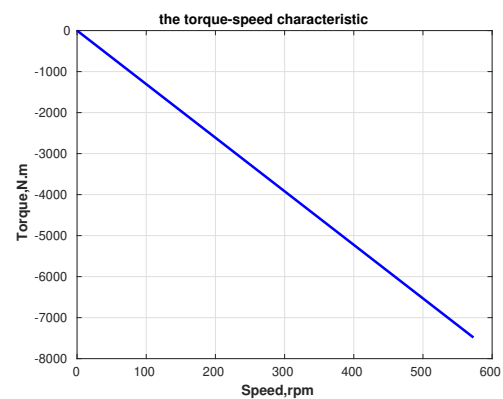


Fig. 11. Speed Torque Characteristics

settling time of 0.03 seconds, out any appreciable overshoot

and zero steady state error in speed shown in Figure V. Also phase currents are settling to steady state, when actual current reaches the reference current. From the above shows the speed response of the BLDC drive with conventional PI controller response of the drive is slower than that of FLC speed controller. The former controller shows an overshoot in speed response, which is undesirable. The drive takes maximum permissible current to start the motor from standstill. The results prove that the response of the drive is faster with FLC controller than the conventional PI controller. Improved response in case of FLC controller is of immense help to industrial applications.

The simulation result for speed reference input of 700 rpm with a load torque of 0.7 N-m are shown in Figure V. The controller gains are $K_p = 0.8$, $K_i = 0.02$ and current controller bandwidth is 0.3A. The rotor is standstill at time zero with onset of the speed reference, the speed error, torque reference, and attains maximum value. The current is made to follow the reference by the current controller. Therefore electromagnetic follows the reference value.

VI. CONCLUSION

A fuzzy logic controller (FLC) has been employed for the speed control of brushless DC motor drive and analysis of results of the performance of a fuzzy controller is presented. The modelings and simulation of the complete drive system is described in this thesis. Effectiveness of the model is established by performance prediction over a wide range of operating conditions. A performance comparison between the fuzzy logic controller and the conventional PI controller has been carried out by simulation runs confirming the validity and superiority of the fuzzy logic controller for implementing the fuzzy logic controller to be adjusted such that manual tuning time of the classical controller is significantly reduced. The performance of the brushless DC motor drive with reference to PI controller, FLC controller and experimental verified with conventional PI controller using DSP processor. Fuzzy logic speed controller improved the performance of brushless DC motor drive of the fuzzy logic speed controller.

REFERENCES

- [1] G. Andrieux and T. Taufer, "Drive a brushless dc motor like a standard dc motor," *ATZelektronik worldwide*, vol. 11, no. 5, pp. 58–63, Oct 2016. [Online]. Available: <https://doi.org/10.1007/s38314-016-0076-9>
- [2] P. C. Krause, O. Wasynczuk, and S. D. Sudhoff, *Brushless dc Motor Drives*. IEEE, 2002. [Online]. Available: <https://doi.org/10.1109/9780470544167.ch15>
- [3] S. Biwersi, S. Tavernier, and S. Equoy, "Electric compressor with high-speed brushless dc motor," *MTZ worldwide*, vol. 73, no. 12, pp. 50–53, Dec 2012. [Online]. Available: <https://doi.org/10.1007/s38313-012-0252-0>
- [4] V. V. Kochergin and B. V. Zakrevskaya, "Ac-based brushless dc motor," *Russian Electrical Engineering*, vol. 80, no. 10, pp. 539–541, Oct 2009. [Online]. Available: <https://doi.org/10.3103/S1068371209100046>
- [5] P. Dessante, J. Vannier, and C. Ripoll, "Optimization of a linear brushless dc motor drive," in *Recent Developments of Electrical*

- Drives*, S. Wiak, M. Dems, and K. Komeza, Eds. Dordrecht: Springer Netherlands, 2006, pp. 127–136.
- [6] H. Tan, J.-z. Jiang, X.-y. Wang, and Y. Wang, "A novel current sensor technique for brushless dc motor drives," *Journal of Shanghai University (English Edition)*, vol. 4, no. 1, pp. 42–48, Mar 2000. [Online]. Available: <https://doi.org/10.1007/s11741-000-0030-0>
- [7] W. Thomson, *Theory of vibration with applications*. CrC Press, 2018.
- [8] S. Chapman, *Electric machinery fundamentals*. Tata McGraw-Hill Education, 2005.
- [9] S. P. Singh, K. K. Singh, and B. Kumar, "Performance evaluation of brushless dc motor drive supplied from hybrid sources," in *Applications of Artificial Intelligence Techniques in Engineering*, H. Malik, S. Srivastava, Y. R. Sood, and A. Ahmad, Eds. Singapore: Springer Singapore, 2019, pp. 443–453.
- [10] A. Sinha, S. K. Bharti, A. K. Samantaray, G. Chakraborty, and R. Bhattacharyya, "Sommerfeld effect in an oscillator with a reciprocating mass," *Nonlinear Dynamics*, vol. 93, no. 3, pp. 1719–1739, Aug 2018. [Online]. Available: <https://doi.org/10.1007/s11071-018-4287-x>
- [11] G. R. Puttalakshmi and S. Paramasivam, "Mathematical modeling of bldc motor using two controllers for electric power assisted steering application," in *Power Electronics and Renewable Energy Systems*, C. Kamalakannan, L. P. Suresh, S. S. Dash, and B. K. Panigrahi, Eds. New Delhi: Springer India, 2015, pp. 1437–1444.
- [12] Zhaojun Meng, Rui Chen, Changzhi Sun, and Yuejun An, "The mathematical simulation model of brushless dc motor system," in *2010 International Conference on Computer Application and System Modeling (ICCASM 2010)*, vol. 12, Oct 2010, pp. V12–625–V12–629. [Online]. Available: <https://doi.org/10.1109/ICCASM.2010.5622430>
- [13] D. Sun, X. Cheng, and X. Xia, "Research of novel modeling and simulation approach of brushless dc motor control system," in *2010 International Conference on E-Product E-Service and E-Entertainment*, Nov 2010, pp. 1–5. [Online]. Available: <https://doi.org/10.1109/ICEEE.2010.5661384>
- [14] G. Qi, "Energy cycle of brushless dc motor chaotic system," *Applied Mathematical Modelling*, vol. 51, pp. 686–697, 2017. [Online]. Available: <https://doi.org/10.1016/j.apm.2017.07.025>
- [15] K. Andanapalli and B. R. K. Varma, "Park's transformation based symmetrical fault detection during power swing," in *2014 Eighteenth National Power Systems Conference (NPSC)*, Dec 2014, pp. 1–5. [Online]. Available: <https://doi.org/10.1109/NPSC.2014.7103817>
- [16] G. Sturtzer, D. Flieller, and J.-P. Louis, "Reduction of torque undulation and extension of the park's transformation applied to non-sinusoidal saturated synchronous motors," *Mathematics and Computers in Simulation*, vol. 63, no. 3, pp. 297–305, 2003, modelling and Simulation of Electric Machines, Converters and Systems. [Online]. Available: [https://doi.org/10.1016/S0378-4754\(03\)00077-6](https://doi.org/10.1016/S0378-4754(03)00077-6)
- [17] P. Wach, *Brushless DC Motor Drives (BLDC)*. Berlin, Heidelberg: Springer Berlin Heidelberg, 2011, pp. 281–380. [Online]. Available: https://doi.org/10.1007/978-3-642-20222-3_4
- [18] A. Rodríguez-Molina, M. G. Villareal-Cervantes, and M. Aldape-Pérez, "An adaptive control study for the dc motor using meta-heuristic algorithms," *Soft Computing*, Aug 2017. [Online]. Available: <https://doi.org/10.1007/s00500-017-2797-y>
- [19] M. Eremia, C.-C. Liu, and A.-A. Edris, *Heuristic Optimization Techniques*. IEEE, 2016. [Online]. Available: <https://doi.org/10.1002/9781119175391.ch21>
- [20] N. F. O. Serteller and D. Ustundag, "Analysis of dynamic behavior of direct current motor with electrical braking techniques," in *2017 CHILEAN Conference on Electrical, Electronics Engineering, Information and Communication*

- Technologies (CHILECON)*, Oct 2017, pp. 1–7. [Online]. Available: <https://doi.org/10.1109/CHILECON.2017.8229542>
- [21] B. K. Bose and R. L. Steigerwald, "A dc motor control system for electric vehicle drive," *IEEE Transactions on Industry Applications*, vol. IA-14, no. 6, pp. 565–572, Nov 1978. [Online]. Available: <https://doi.org/10.1109/TIA.1978.4503593>
- [22] M. Ceraolo and D. Poli, *Electric Machines and Static Converters*. IEEE, 2014. [Online]. Available: <https://doi.org/10.1002/9781118922583.part3>
- [23] M. Ceraolo and D. Poli, *DC Machines and Drives and Universal Motors*. IEEE, 2014. [Online]. Available: <https://doi.org/10.1002/9781118922583.ch10>
- [24] M. Sato, G. Yamamoto, D. Gunji, T. Imura, and H. Fujimoto, "Development of wireless in-wheel motor using magnetic resonance coupling," *IEEE Transactions on Power Electronics*, vol. 31, no. 7, pp. 5270–5278, July 2016. [Online]. Available: <https://doi.org/10.1109/TPEL.2015.2481182>
- [25] M. Kato, T. Imura, and Y. Hori, "New characteristics analysis considering transmission distance and load variation in wireless power transfer via magnetic resonant coupling," in *Intelec 2012*, Sept 2012, pp. 1–5. [Online]. Available: <https://doi.org/10.1109/INTLEC.2012.6374474>
- [26] *Feedforward Control and PD Control plus Feedforward*. London: Springer London, 2005, pp. 263–285. [Online]. Available: https://doi.org/10.1007/1-85233-999-3_15
- [27] K. Rajagopal, S. Vaidyanathan, A. Karthikeyan, and P. Duraisamy, "Dynamic analysis and chaos suppression in a fractional order brushless dc motor," *Electrical Engineering*, vol. 99, no. 2, pp. 721–733, Jun 2017. [Online]. Available: <https://doi.org/10.1007/s00202-016-0444-8>
- [28] C. Weiß, *Lyapunov Exponents*. Cham: Springer International Publishing, 2014, pp. 127–133. [Online]. Available: https://doi.org/10.1007/978-3-319-04075-2_8
- [29] J. C. Vallejo and M. A. F. Sanjuan, *Lyapunov Exponents*. Cham: Springer International Publishing, 2017, pp. 25–59. [Online]. Available: https://doi.org/10.1007/978-3-319-51893-0_2
- [30] V. A. Trenogin, "The lyapunov theorem on stability with respect to linear approximation as a corollary to the implicit operator theorem," *Doklady Mathematics*, vol. 73, no. 2, pp. 292–295, Jun 2006. [Online]. Available: <https://doi.org/10.1134/S1064562406020360>
- [31] M. Johansson, *Lyapunov Stability*. Berlin, Heidelberg: Springer Berlin Heidelberg, 2003, pp. 41–84. [Online]. Available: https://doi.org/10.1007/3-540-36801-9_4
- [32] B. N. N. Achar, C. F. Lorenzo, and T. T. Hartley, *The Caputo Fractional Derivative: Initialization Issues Relative to Fractional Differential Equation*. Dordrecht: Springer Netherlands, 2007, pp. 27–42. [Online]. Available: https://doi.org/10.1007/978-1-4020-6042-7_3
- [33] D. Tavares, R. Almeida, and D. F. Torres, "Caputo derivatives of fractional variable order: Numerical approximations," *Communications in Nonlinear Science and Numerical Simulation*, vol. 35, pp. 69–87, 2016. [Online]. Available: <https://doi.org/10.1016/j.cnsns.2015.10.027>
- [34] C. Li, D. Qian, and Y. Chen, "On riemann-liouville and caputo derivatives," *Discrete Dynamics in Nature and Society*, vol. 2011, pp. 1–15, 2011. [Online]. Available: <http://dx.doi.org/10.1155/2011/562494>
- [35] T. Abdeljawad, "On riemann and caputo fractional differences," *Computers & Mathematics with Applications*, vol. 62, no. 3, pp. 1602–1611, 2011, special Issue on Advances in Fractional Differential Equations II. [Online]. Available: <http://www.sciencedirect.com/science/article/pii/S089812211100188X>
- [36] A. Bisoi, A. Samantaray, and R. Bhattacharyya, "Control strategies for dc motors driving rotor dynamic systems through resonance," *Journal of Sound and Vibration*, vol. 411, pp. 304–327, 2017. [Online]. Available: <https://doi.org/10.1016/j.jsv.2017.09.014>
- [37] S. Junco, A. Donaire, and G. Garnero, "Speed control of series dc motor: a bond graph based backstepping design," in *IEEE International Conference on Systems, Man and Cybernetics*, vol. 3, Oct 2002, pp. 6 pp. vol.3–. [Online]. Available: <https://doi.org/10.1109/ICSMC.2002.1176035>
- [38] M. Bodson and J. Chiasson, "Differential-geometric methods for control of electric motors," *International Journal of Robust and Nonlinear Control*, vol. 8, no. 11, pp. 923–954. [Online]. Available: [https://doi.org/10.1002/\(SICI\)1099-1239\(199809\)8:11%3C923::AID-RNC369%3E3.0.CO;2-S](https://doi.org/10.1002/(SICI)1099-1239(199809)8:11%3C923::AID-RNC369%3E3.0.CO;2-S)